Materials Research Express

OPEN ACCESS

RECEIVED
8 November 2021

REVISED
8 December 2021

ACCEPTED FOR PUBLICATION
15 December 2021

PUBLISHED
24 December 2021

PAPER

Magnetic competition in topological kagome magnets

Thanh-Mai Thi Tran[1], Duong-Bo Nguyen[2], Hong-Son Nguyen[3] and Minh-Tien Tran[1]

[1] Institute of Physics, Vietnam Academy of Science and Technology, Hanoi 10000, Vietnam
[2] Graduate University of Science and Technology, Vietnam Academy of Science and Technology, Hanoi 10000, Vietnam
[3] Department of Occupational Safety and Health, Trade Union University, Hanoi 10000, Vietnam

E-mail: minhtien@iop.vast.vn

Keywords: electron correlations, kagome lattice, magnetic phase transition, topological insulator

Abstract

Magnetic competition in topological kagome magnets is studied by incorporating the spin–orbit coupling, anisotropic Hund coupling and spin exchange into a tight-binding electron dynamics in the kagome lattice. Using the Bogoliubov variational principle we find the stable phases at zero and finite temperatures. At zero temperature and in the strong Ising-Hund coupling regime, a magnetic tunability from the out-of-plane ferromagnetism to the in-plane antiferromagnetism is achieved through a universal property of the critical in-plane Hund coupling. At low temperature the out-of-plane ferromagnetism is stable until a finite crossing temperature. Above the crossing temperature the in-plane antiferromagnetism is stable, but the magnetization of the out-of-plane ferromagnetism still survives. This suggests a metastable coexistence of these magnetic phases in a finite temperature range. A large anomalous Hall conductance is observed in the Ising-Hund coupling limit.

1. Introduction

The emergent phases resulting from the interplay between magnetism, correlations and topology are the subject of intense research interest because of their intriguing properties and substantial interest for spintronic technologies. The kagome lattice, a two-dimensional network of corner-sharing triangles, offers a versatile platform to study such phases, because with the special lattice geometry it can host peculiar states including unconventional magnetism [1–3], nontrivial topology [4, 5], flat band [6], Dirac electrons [7], quantum spin liquids [8]. With the inclusion of electron correlations and spin–orbit coupling (SOC), the kagome lattice engenders a rich interplay between unconventional magnetism, electron correlations and nontrivial topology. Recently, experiments observed striking effects including large anomalous Hall effect and unusual magnetic tunability in magnetic kagome materials [9–13]. In particular, the kagome magnet $Co_3Sn_2S_2$ exhibits an out-of-plane ferromagnetic (FM) ground state, but at a finite temperature before reaching the paramagnetic (PM) state an in-plane antiferromagnetism (AFM) appears and coexists with the out-of-plane FM [12, 13]. The competition between these magnetic phases is tunable through applying either an external magnetic field or hydrostatic pressure [12, 13].

The present work is motivated by the striking effects observed in the kagome magnets, and in particular, the magnetic competition between the out-of-plane FM and the in-plane AFM [9–13]. We propose a minimal model, which can qualitatively describe the observed effects. The model is generally applied to the family of kagome magnets, but we particularly focus on the $Co_3Sn_2S_2$ magnet. Because the magnetic Co atoms form a kagome lattice in the *xy*-plane, the proposed model is built on the two-dimensional kagome lattice. It describes a system of itinerant electrons coupled with localized spins. The coupling is essentially an anisotropic Hund one. In addition, the model also includes the SOC of itinerant electrons, and an anisotropic spin exchange (SE) between the localized spins. The Hund coupling can generate the double exchange processes between itinerant electrons and localized spins, and as a result a long-range magnetic ordering may be established [14, 15]. The anisotropic SE on the kagome lattice can induce a magnetic competition between out-of-plane and in-plane magnetic orderings of the localized spins [1–3]. As a consequence, the double exchange processes also depend on the magnetic competition. The interplay between the Hund coupling and the SE in the presence of the SOC

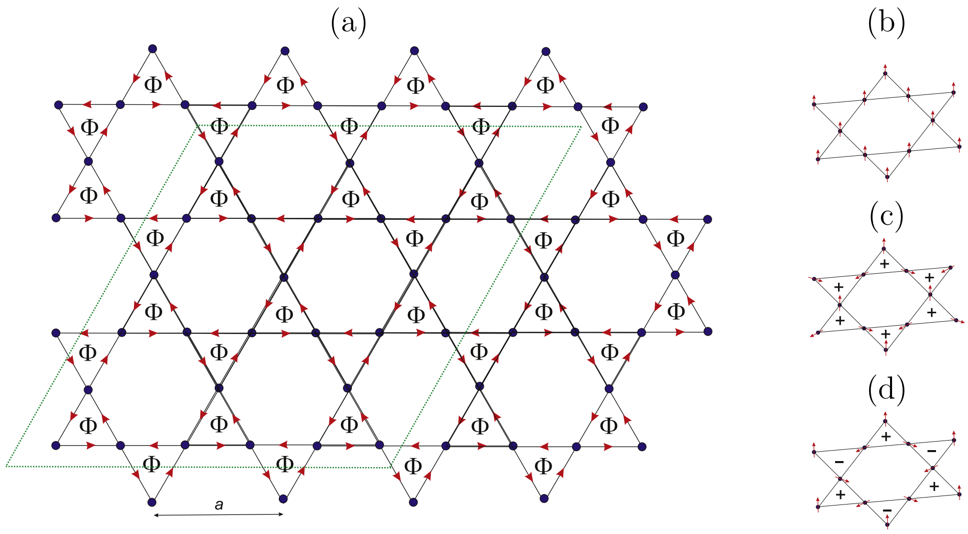

Figure 1. (a) Kagome lattice. The arrows on bonds mean the sign $\nu_{ij} = 1$ of the SOC. Φ is the flux penetrating each triangle. The green dotted rhombus is the 3×3 unit cell. (b) Out-of-plane FM state. (c) & (d) In-plane 1×1 and $\sqrt{3} \times \sqrt{3}$ AFM states, respectively. The signs $\pm$ indicate the spin chirality $\chi = \pm 1$ of each triangle. The lattice parameter $a = 1$.

could intriguingly impact on the magnetic competition and the topology of the system. We will use the Bogoliubov variational principle to find the stable phases resulting from the interplay [16, 17]. The Bogoliubov variational principle selects the phase with lowest free energy among a phase family of a proposed phase ansatz. We find indeed a magnetic competition between the out-of-plane FM and the in-plane AFM. The magnetic competition occurs across a magnetic tunability, which is achieved through a universal property of the critical coupling. At low temperature the out-of-plane FM is stable until a crossing temperature, above which the in-plane AFM is stable. However, the out-of-plane FM magnetization does not vanish in the in-plane AFM phase. This suggests a metastable coexistence of the out-of-plane FM and the in-plane AFM in a finite temperature range. In the Ising-Hund coupling limit, a large anomalous Hall conductance is also observed at the magnetic phase transition.

The plan of the present paper is as follows. In section 2 we describe the proposed model. The numerical results are presented in section 3. Section 4 is the conclusion.

2. Model

The kagome magnets have a layered crystal structure with stacked quasi-two-dimensional kagome layers [10–13]. We focus on the two-dimensional kagome lattice, where the magnetic atoms are located in the kagome lattice sites (see figure 1). For instance, in the $Co_3Sn_2S_2$ magnet, the magnetic Co atoms form the kagome lattice in the xy-plane. Magnetism of Co atoms can be realized through their localized spins located in the kagome lattice sites, reflecting strong correlations of the Co $3d$ orbitals in the Mott regime [18, 19]. In general, the SE between the localized spins can be anisotropic [3]. Itinerant electrons come from the Sn $5p$ orbitals. The itinerant electrons are coupled with the localized spins through an anisotropic Hund coupling. The Hamiltonian describing the kagome magnets reads

$$H = -t \sum_{\langle i,j \rangle,\sigma} c^{\dagger}_{i\sigma} c_{j\sigma} - i\lambda \sum_{\langle i,j \rangle,s,s'} \nu_{ij} c^{\dagger}_{is} \sigma^{z}_{ss'} c_{js'} - \sum_{i,\alpha,ss'} h_{\alpha} S^{\alpha}_{i} c^{\dagger}_{is} \sigma^{\alpha}_{ss'} c_{is'} - \sum_{\langle i,j \rangle,\alpha} J_{\alpha} S^{\alpha}_{i} S^{\alpha}_{j}, \quad (1)$$

where $c^{\dagger}_{i\sigma}$ ($c_{i\sigma}$) is the creation (annihilation) operator for electron with spin σ at site i. $\langle i, j \rangle$ denote the nearest-neighbor lattice sites. t is the hopping parameter. The SOC is introduced through the direction-dependent hopping and λ is its strength. The sign $\nu_{ij} = \pm 1$ when the hopping of the SOC is counterclockwise (clockwise). σ^{α} is the Pauli matrix ($\alpha = x, y, z$). The first two terms in Hamiltonian (1) describes the band structure of itinerant electrons in the presence of their SOC. They are essentially the Kane-Mele model on the kagome lattice, and would describe a Z_2 topological insulator [20]. S^{α}_{i} is the α-component of localized spin at lattice site i, and without loss of generality it is renormalized that $\mathbf{S}^2_i = 1$. h_{α} is the α-component of the Hund coupling between the itinerant and localized electrons. J_{α} is the SE between the nearest-neighbor localized spins in the α-direction. In general, we consider the case where the Hund coupling and the SE are isotropic in plane $h_x = h_y \equiv h_{xy}$,

$J_x = J_y \equiv -J_{xy}$, but anisotropic out of plane $h_z \neq h_{xy}$, $J_z \neq J_{xy}$. Note that the SE in plane J_{xy} and out of plane J_z have the opposite signs [3]. The Hund coupling essentially describes the double exchange processes between itinerant electrons and localized spins [14, 15]. As widely adopted in the studies of magnetic materials, we will treat the localized spins classically [14, 15, 21–32].In addition, we omit the nearest-neighbor interactions between itinerant electrons and localized spins. They would be weaker than the local Hund coupling. In the double-exchange processes, the Hund coupling is dominant and the localized spins are ordered to minimize the kinetic energy. The nearest-neighbor interactions may impact on the magnetic ordering, but not significantly at least in the mean-field approximation. The SE part of Hamiltonian in (1) is just the Heisenberg XXZ model [1, 2]. For classical spins the XXZ model produces a magnetic phase transition from the out-of-plane FM to an in-plane magnetic state at $J_{xy} = 2J_z$ [1–3]. In the out-of-plane FM all spins are parallel to the z-axis, while in the in-plane states, they are all in the xy-plane. The in-plane states are macroscopically degenerate. Any state with all spins pointing along one of three directions mutually oriented at 120° can be the ground state [1, 2]. We will refer them as in-plane 120° states. These in-plane states resemble the set of the ground states of the three-state Potts model [33]. However, the thermal or quantum fluctuations can remove the macroscopic degeneracy [1, 2]. As we will see later, the in-plane Hund coupling can also remove the degeneracy even when the spins are classical. The model in the Ising-Hund coupling limit $h_{xy} = 0$ was previously proposed [3].

The tight-binding part of Hamiltonian (1) can be rewritten as

$$H_{QSH} = -\sum_{\langle i,j\rangle,\sigma} t_{ij\sigma} c_{i\sigma}^{\dagger} c_{j\sigma}, \tag{2}$$

where $t_{ij\sigma} = t + i\nu_{ij}\sigma\lambda = r\exp(\pm i\Phi/3)$ with $r = \sqrt{t^2 + \lambda^2}$, and $\Phi = 3\arg(t + i\lambda)$. In the following we use $r = 1$ as the energy unit. The quantity Φ can be interpreted as a magnetic flux penetrating each triangle of the kagome lattice (see figure 1(a)). It ($\Phi \neq 0, \pi$) induces topologically nontrivial band structure [4, 5]. When the Hund coupling is included, its interplay with the SOC can emerge topological magnetic phases [31, 32]. Hamiltonian (2) is just the spin version of the quantum anomalous Hall model, which is obtained from the double exchange model in the strong Hund coupling limit [4]. The Hall conductivity C_σ of electrons with spin σ in unit e^2/h can be calculated by the Kubo formula

$$C_\sigma = \frac{1}{N}\sum_{\mathbf{k},a,b} \frac{\Im[\langle \mathbf{k}a|j_x|\mathbf{k}b\rangle\langle \mathbf{k}b|j_y|\mathbf{k}a\rangle]}{(E_{\mathbf{k}a} - E_{\mathbf{k}b})^2}(f(E_{\mathbf{k}a}) - f(E_{\mathbf{k}b})), \tag{3}$$

where j_α is the current operator in α-direction, $|\mathbf{k}a\rangle$ and $E_{\mathbf{k}a}$ are the normalized eigenstate and eigenvalue of the Bloch Hamiltonian of electrons with spin σ, $f(x)$ is the Fermi–Dirac distribution function, and N is the number of lattice sites. At zero temperature $T = 0$, C_σ is just the invariant number of the first Chern class over the Brillouin torus [34, 35]. Hamiltonian (2) for each spin component has three bands separated by two gaps [4]. The insulating state occurs at fillings $n_\sigma = 1/3, 2/3$, and $C_\sigma = \sigma$. At these fillings the charge Hall conductivity $\sigma_{xy}^c = (e^2/h)\sum_\sigma C_\sigma$ vanishes, whereas the spin Hall conductivity $\sigma_{xy}^s = (e^2/h)\sum_\sigma \sigma C_\sigma$ is quantized. This is exactly the quantum spin Hall (QSH) effect proposed in the Z_2 topological insulators [20]. In the present work, we focus on the half filling $n = \sum_\sigma n_\sigma = 1$, because in order to establish the double exchange processes, itinerant electrons need to be movable in the lattice.

3. Numerical results

We will perform variational calculations to find the stable phases. The variational principle is based on the Bogoliubov inequality

$$\Omega \leqslant \Omega_{tr} + \langle H - H_{tr}\rangle_{tr} \equiv \tilde{\Omega}, \tag{4}$$

where Ω, Ω_{tr} are the grand potentials corresponding to the ensembles defined by the studied H and trial H_{tr} Hamiltonians, respectively [16, 17]. The thermodynamical average is taken over the trial ensemble. Minimizing $\tilde{\Omega}$ in equation (4) one would find the stable phases of the studied system.

3.1. Zero temperature

At zero temperature $T = 0$, $\tilde{\Omega} = E - \mu nN$, where μ is the chemical potential, E and n are the ground-state energy and the electron filling of the trial state. In calculating the ground state energy and the electron filling, we use the two-dimensional tetrahedron method to calculate the integration over the Brillouin zone [36]. We consider different trial states, and in particular, the out-of-plane FM state, the in-plane 120° states and the canted 120° states that are generated by the configurations of localized spins within the 3×3 unit cell. The 3×3 unit cell contains 27 lattice sites (see figure 1(a)). Within it there are 120 different 120° configurations of localized spins in the xy-plane [1]. Among these spin configurations, the 1×1 and the $\sqrt{3} \times \sqrt{3}$ AFM ones are most prominent. These AFM states are depicted in figures 1(c), (d). They are defined within the 1×1 and the $\sqrt{3} \times \sqrt{3}$ unit cells. They are distinguishable by the vector chirality of each lattice triangle

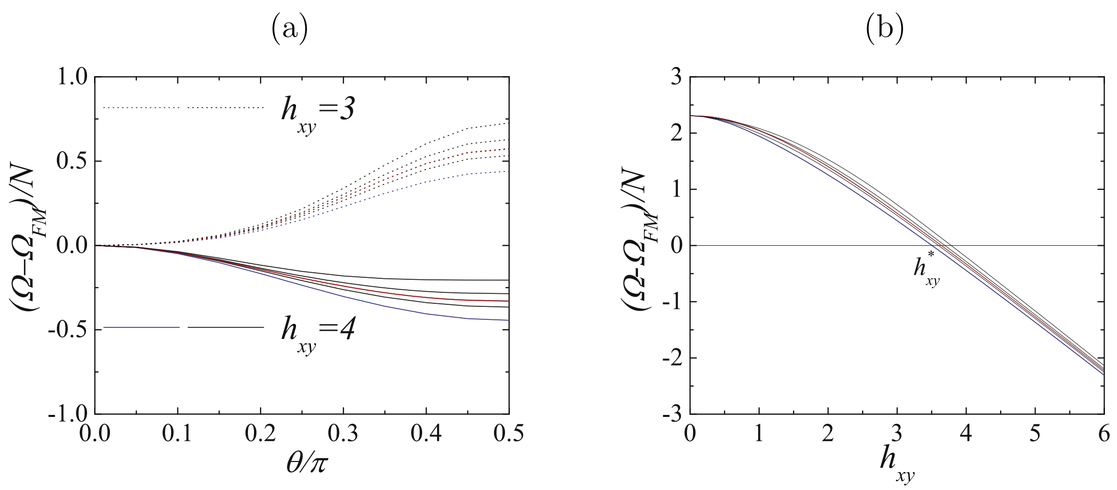

Figure 2. The grand potential $\Omega - \Omega_{FM}$ measured from that of the out-of-plane FM state at zero temperature $T = 0$ and half filling for (a) canted spin states with the polar angle θ and a fixed h_{xy}; (b) in-plane states ($\theta = \pi/2$). The blue (red) lines are the grand potential for the in-plane 1×1 ($\sqrt{3} \times \sqrt{3}$) AFM state. Other model parameters: $h_z = 6, J_z = 1, J_{xy} = 4, \Phi = \pi/3$.

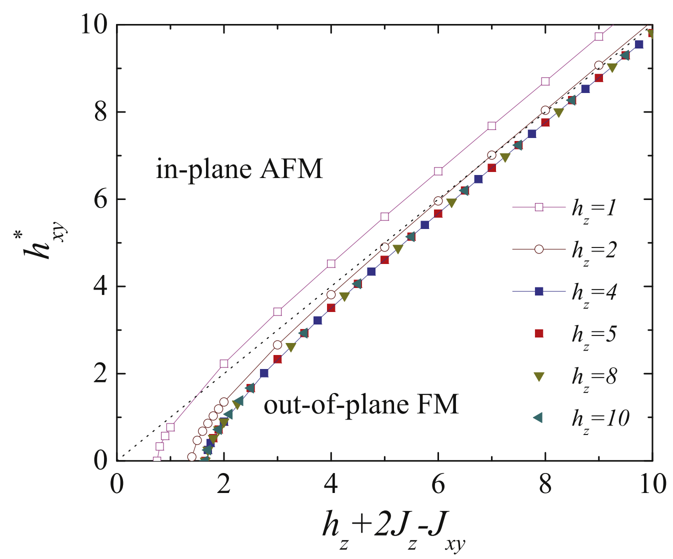

Figure 3. The critical line h^*_{xy} via $(h_z + 2J_z - J_{xy})$ at half filling and flux $\Phi = \pi/3$. The ground state is the out-of-plane FM when $h_{xy} < h^*_{xy}$, and the in-plane AFM when $h_{xy} > h^*_{xy}$. The dotted line is the asymptotic $h^*_{xy} = h_z + 2J_z - J_{xy}$.

$\chi=[2/3\sqrt{3}](\mathbf{S}_1 \times \mathbf{S}_2 + \mathbf{S}_2 \times \mathbf{S}_3 + \mathbf{S}_3 \times \mathbf{S}_1) \equiv \mathbf{e}_z\chi$, which is parallel to the z-axis ($\mathbf{e}_z$ is the unit vector of the z-axis). The 1×1 AFM has the uniform chirality $\chi = 1$, whereas the $\sqrt{3} \times \sqrt{3}$ AFM has the staggered chirality $\chi = \pm 1$. The canted 120° states are the non-coplanar spin states, in which all localized spins have the same polar angle θ, and their projections in the xy-plane form the in-plane 120° states. The canted state with $\theta = 0$ is actually the out-of-plane FM one. When $\theta = \pi/2$, the canted states are the in-plane 120° states.

In figure 2(a) we plot the grand potential of all canted 120° states, defined within the 3×3 unit cell. It shows that the grand potential is minimal at either $\theta = 0$ or $\theta = \pi/2$, or equivalently, the ground state is either the out-of-plane FM or the in-plane 1×1 AFM. Note that the in-plane $\sqrt{3} \times \sqrt{3}$ AFM has a higher grand potential. The in-plane AFM experimentally observed in $Co_3Sn_2S_2$ is the 1×1 one [12, 13]. Figure 2(b) also shows a transition from the out-plane FM to the in-plane 1×1 AFM states when the in-plane Hund coupling h_{xy} varies. The magnetic phase transition occurs at a critical value h^*_{xy}. When $h_{xy} < h^*_{xy}$, the out-of-plane FM is stable, and when $h_{xy} > h^*_{xy}$ the in-plane 1×1 AFM is stable, because their grand potential has a lowest value. We have also checked the finding with other variational configurations of localized spins.

The phase diagram is summarized in figure 3. In the regime of strong Ising-Hund coupling ($h_z > 3$) we observed that the critical value h^*_{xy} is a universal function of $\Delta h_z \equiv h_z + 2J_z - J_{xy}$ in the sense that h^*_{xy} is independent on details of h_z, J_z, J_{xy}, but their combination Δh_z, as shown in figure 3. The critical line $h^*_{xy}(\Delta h_z)$ approaches the asymptotic $h^*_{xy} = \Delta h_z$ at large Δh_z. The universal property of $h^*_{xy}(\Delta h_z)$ suggests the equivalence

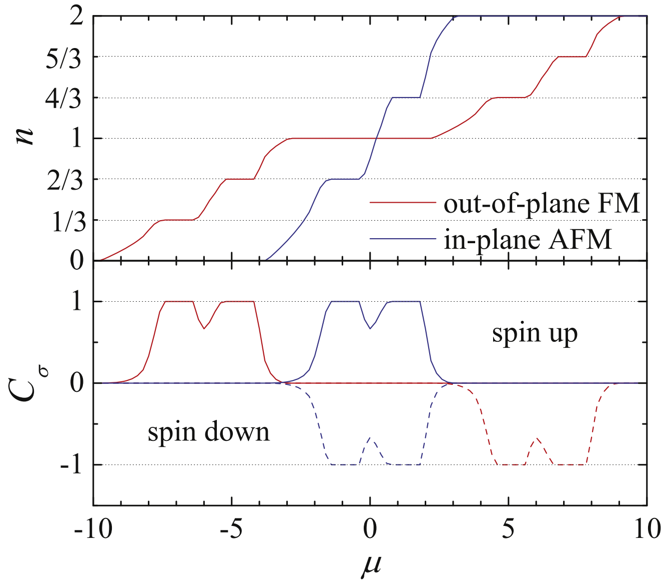

Figure 4. The electron filling n and the spin components of the Hall conductivity C_σ in unit e^2/h via the chemical potential μ at zero temperature $T = 0$ in the Ising-Hund coupling limit $h_{xy} = 0$. Model parameters $h_z = 6, \Phi = \pi/3$.

between the Hund coupling and the SE, as well as between their out-of-plane and in-plane components in the magnetic competition. Due to the universal property, the magnetic phase transition from the out-of-plane FM to the in-plane AFM states is tunable through tuning the components of either the Hund coupling or the SE. This also allows us to drop the SE in studying the magnetic phase transition when h_z is strong. Without the SE, the many-body local methods such as the dynamical mean field theory can safely be used [37]. Actually, the SE can be generated by the Hund coupling through the Ruderman-Kittel-Kasuya-Yosida mechanism, and it is already implicitly present in the models having the Hund coupling [38–40]. The universal function $h^*_{xy}(\Delta h_z)$ also implies us that the kagome magnets with strong Ising-Hund coupling form a common family of materials, where the magnetic phase transition from out-of-plane to the in-plane magnetisms is flexibly tunable and does not depend on specific values of the Hund coupling and the SE as long as Δh_z is fixed. The magnetic tunability observed in $Co_3Sn_2S_2$ suggests that this kagome magnet has a strong anisotropic Hund coupling and may belong to the suggested family of materials [12, 13]. Experiments also observed that $Co_3Sn_2S_2$ in the FM phase exhibits unconventional critical behaviors, which suggest an anomalous magnetic state below the FM critical temperature [41]. The anomalous magnetic state may be relevant to the flexible magnetic tunability between the out-of-plane FM and the in-plane AFM phases.

From the universal property of $h^*_{xy}(\Delta h_z)$, one can see that the magnetic phase transition still occurs in the Ising-Hund coupling limit $h_{xy} = 0$, providing J_{xy} with tunability [3]. In this limit, the Bloch Hamiltonian of itinerant electrons in a fixed configuration of localized spins is diagonal in the spin index. Therefore, the Hall conductivity can be separated into the spin-component C_σ, which can still be calculated by the Kubo formula (3). Both the electron filling and the Hall conductivity are independent of the SE. However, the SE affects the ground-state energy, and it can drive the magnetic phase transition. In figure 4 we plot the electron filling and the spin components of the Hall conductivity as a function of the chemical potential at $T = 0$. It shows that the out-of-plane FM state has quantized $C_\sigma = \pm 1$ at fillings $n = 1/3, 2/3, 4/3, 5/3$ and the in-plane AFM has quantized $C_\sigma = \sigma$ at fillings $n = 2/3, 4/3$. Therefore, the charge Hall conductivity σ^c_{xy} is only quantized in the out-of-plane FM and vanishes in the in-plane AFM. However, the spin Hall conductivity σ^s_{xy} is quantized in the in-plane AFM. Nearby half filling, both the charge and spin Hall conductivities in the out-of-plane FM vanish. However, the spin Hall conductivity in the in-plane AFM is finite, although it is not quantized. It yields a large anomalous spin Hall conductance because $e^2/ha \sim 717\ \Omega^{-1}\ \mathrm{cm}^{-1}$ with typical lattice parameter $a \sim 5.4$ Å [10]. The finite value of the spin Hall conductivity at half filling results from an interference of two quantum spin Hall conductivities at fillings $n = 2/3$ and $n = 4/3$. This finding indicates that a large anomalous spin Hall conductance may be observed at half filling in the in-plane AFM.

3.2. Finite temperature

At finite temperature we use the following trial Hamiltonian in the Bogoliubov variational calculation

$$H_{tr} = H^c_{tr} + H^S_{tr}, \tag{5}$$

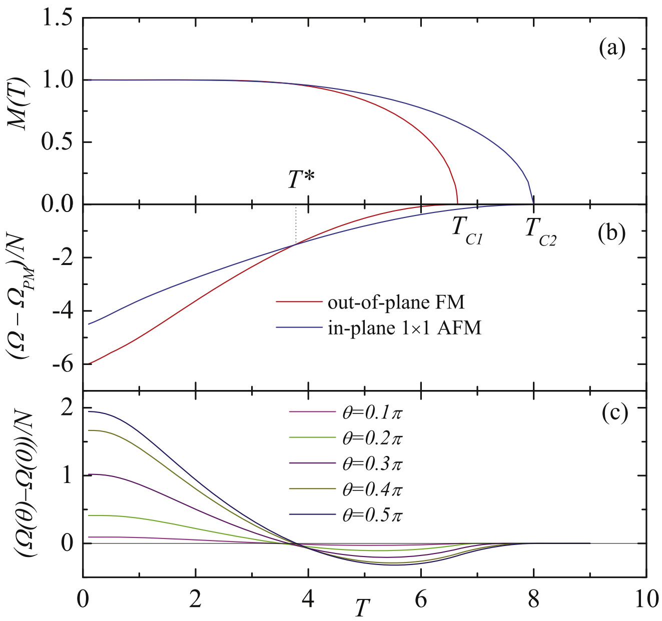

Figure 5. (a) The out-of-plane FM and the in-plane 1×1 AFM magnetizations $M(T)$ via temperature T. (b) The grand potential $\Omega - \Omega_{PM}$ measured from that of the PM state via temperature T. (c) The grand potential $\Omega(\theta) - \Omega(0)$ measured from that of the out-of-plane FM ($\theta = 0$) via temperature T. T^* is the temperature below which the out-of-plane FM is stable. T_{C1} and T_{C2} are the critical temperatures, where the out-of-plane FM and the in-plane AFM magnetizations respectively vanish. Model parameters $h_z = 6$, $h_{xy} = 1, J_z = 1, J_{xy} = 4, \Phi = \pi/3$ and half filling $n = 1$.

$$H^c_{tr} = -t \sum_{\langle i,j \rangle \sigma} c^\dagger_{i\sigma} c_{j\sigma} - i\lambda \sum_{\langle i,j \rangle, ss'} \nu_{ij} c^\dagger_{is} \sigma^z_{ss'} c_{js'} - \sum_{i,ss',a} U^a_i c^\dagger_{is} \sigma^a_{ss'} c_{is'}, \tag{6}$$

$$H^S_{tr} = -\sum_{i,ss',a} V^a_i S^a_i, \tag{7}$$

where $\mathbf{U}_i$ and $\mathbf{V}_i$ are the local mean fields acting on the itinerant electron and localized spins, respectively. The trial Hamiltonian (5) disentangles the itinerant electrons and the localized spins in a mean field approximation. In order to describe both the out-of-plane FM and the in-plane AFM phases, the following ansatzs for the local mean fields at the 3 sites of the triangles in the kagome lattice

$$\mathbf{Z}_1 = M_Z(T)\left(-\frac{\sqrt{3}}{2}\sin\theta,\ -\frac{1}{2}\sin\theta,\ \cos\theta\right), \tag{8}$$

$$\mathbf{Z}_2 = M_Z(T)\left(\frac{\sqrt{3}}{2}\sin\theta,\ -\frac{1}{2}\sin\theta,\ \cos\theta\right), \tag{9}$$

$$\mathbf{Z}_3 = M_Z(T)(0,\ \sin\theta,\ \cos\theta), \tag{10}$$

are used. Here $\mathbf{Z}$ indicates the local mean fields $\mathbf{U}\,\mathbf{V}$, and θ is the polar angle of the mean fields. The ansatz gives the out-of-plane FM when $\theta = 0$, and the in-plane 1×1 AFM when $\theta = \pi/2$. When $\theta \neq 0, \pi/2$, it describes the canted 120° spin structure, the projection of which in the xy-plane forms the in-plane AFM. Both local mean fields acting on the itinerant electron and localized spins have the same ansatz, but with different amplitudes $M_Z(T)$, reflecting the effect of the strong Hund coupling [14]. A mean-field solution is obtained by minimizing the variational $\tilde{\Omega}$ in the Bogoliubov inequality (4) with respect to $M_U(T)$ and $M_V(T)$

$$\frac{\partial\tilde{\Omega}}{\partial M_U} = 0, \qquad \frac{\partial\tilde{\Omega}}{\partial M_V} = 0. \tag{11}$$

Once the mean-field solution is found, the magnetization is calculated by $M(T) = |\langle \mathbf{S} \rangle|$.

In figure 5 we plot the variational solutions for the out-of-plane FM and the in-plane AFM phases at half filling. It shows that below a crossing temperature T^*, where the grand potentials of the out-of-plane FM and of the in-plane AFM phases are equal, the out-of-plane FM phase has a lower grand potential, therefore it is stable in the temperature range $T < T^*$. However, at the crossing temperature T^* the magnetization $M(T)$ of the out-of-plane FM ordering does not vanish. When temperature increases, it decreases and vanishes at the critical temperature $T_{C1} > T^*$. The AFM phase is stable from the crossing temperature T^* until the critical temperature $T_{C2} > T_{C1}$. At temperature $T > T_{C2}$ the PM phase is stable. In the temperature range $T^* < T < T_{C1}$, the AFM phase is stable, but the magnetization of the out-of-plane FM ordering is still finite. We interpret this temperature range as the region of metastable coexistence of the out-of-plane FM and the in-plane AFM phases.

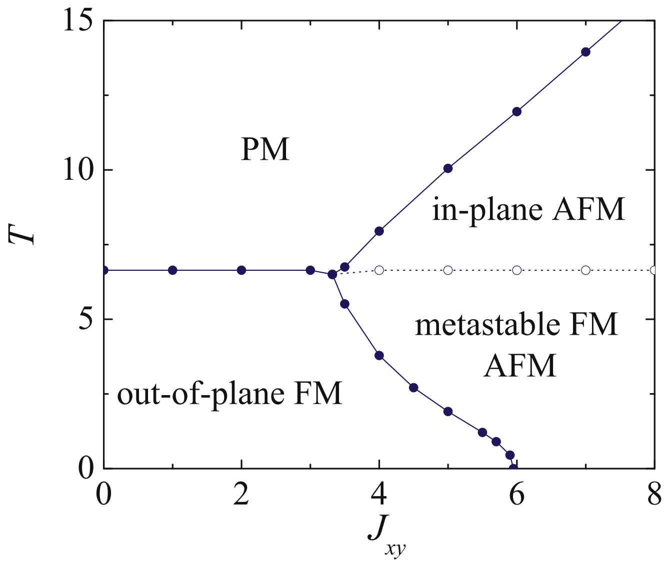

Figure 6. Phase diagram at finite temperature. Model parameters h_z=6, $h_{xy} = 1$, $J_z = 1$, $\Phi = \pi/3$ and half filling $n = 1$.

A recent muon-spin rotation study observed the coexistence of the in-plane AFM and the out-of-plane FM orderings in a finite temperature range [12, 13]. The phase transition from the out-of-plane FM to the in-plane AFM occurs at the crossing point T^*, which is infinitely degenerate, as can be seen in figure 5(c). At the crossing point, any canted phase with any θ has the same grand potential. Therefore, the magnetic phase transition is continuous, although the order parameter does not vanish. Without such infinitely degenerate crossing point, the phase transition from out-of-plane to in-plane magnetism would abruptly occur. The two critical temperatures of the FM and the AFM orderings were also detected by experiments [12, 13]. In undoped $Co_3Sn_2S_2$, T_{C1} and T_{C2} are close that the experimental measurements of the out-of-plane and the in-plane magnetizations did not detect their difference [42]. However, there is a signal of suppression of the out-of-plane FM magnetization at temperature T^* [42]. In doped case, the critical temperatures T_{C1} and T_{C2} are significantly distinct [13]. A typical phase diagram at finite temperature is plotted in figure 6. There is a finite region of J_{xy}, where the ground state is the out-of-plane FM, but when temperature increases the metastable FM phase coexists with the in-plane AFM phase. When the magnetization of the out-of-plane FM vanishes, the in-plane AFM phase is stable until the PM phase is reached. The magnetic competition and the phase transition between the FM and the AFM phases were also observed in perovskite manganites at some dopings, where the FM magnetization is suppressed at the Neel temperature [43].

4. Conclusion

We have studied the interplay between the SOC, the Hund coupling and the SE in the kagome lattice. It causes the magnetic competition between the out-of-plane FM and the in-plane AFM orderings. The magnetic competition qualitatively describes striking effects observed in the kagome magnets, including the magnetic tunability, the large anomalous Hall conductance, the coexistence of the out-of-plane FM and the in-plane AFM orderings in a finite temperature range. At finite temperature the magnetic phase transition is continuous although the order parameter does not vanish. In the present work, quantum corrections to the mean field solution are not considered yet. They may generate topological magnetic excitations, which may impact on the interplay between the SOC, the Hund coupling and the SE. We leave this problem for a further study.

Acknowledgments

This research is funded by Vietnam National Foundation for Science and Technology Development (NAFOSTED) under Grant No 103.01-2019.309.

Data availability statement

The data that support the findings of this study are available upon reasonable request from the authors.

ORCID iDs

Minh-Tien Tran https://orcid.org/0000-0001-9579-3936

References

[1] Sachdev S 1992 *Phys. Rev.* B **45** 12377
[2] Reimers J N and Berlinsky A J 1993 *Phys. Rev.* B **48** 9539
[3] Legendre J and Le Hur K 2020 *Phys. Rev. Res.* **2** 022043(R)
[4] Ohgushi K, Murakami S and Nagaosa N 2000 *Phys. Rev.* B **62** R6065
[5] Guo H M and Franz M 2009 *Phys. Rev.* B **80** 113102
[6] Leykam D, Andreanov A and Flach S 2018 *Adv. in Phys.* X **3** 1473052
[7] Mazin I I, Jeschke H O, Lechermann F, Lee H, Fink M, Thomale R and Valenti R 2014 *Nat. Commun.* **5** 4261
[8] Balents L 2010 *Nature* **464** 199
[9] Nakatsuji S, Kiyohara N and Higo T 2015 *Nature* **527** 212
[10] Liu E *et al* 2018 *Nat. Phys.* **14** 1125
[11] Wang Q, Xu Y, Lou R, Liu Z, Li M, Huang Y, Shen D, Weng H, Wang S and Lei H 2018 *Nat. Commun.* **9** 3681
[12] Guguchia Z *et al* 2020 *Nat. Commun.* **11** 559
[13] Guguchia Z *et al* 2021 *Npj Quantum Materials* **6** 50
[14] Zener C 1951 *Phys. Rev.* **82** 403
[15] Dagotto E 2003 *Nanoscale Phase Separation and Colossal Magnetoresistance, Springer Series in Solid-State Sciences* vol 136 (Berlin, Heidelberg: Springer)
[16] Feynman R P 1972 *Statistical Mechanics* (Reading, MA, USA: Addison-Wesley)
[17] Callen H B 1985 *Thermodynamics and an Introduction to Thermostatistics* (New York, USA: Wiley)
[18] Xu Q, Liu E, Shi W, Muechler L, Gayles J, Felser C and Sun Y 2018 *Phys. Rev.* B **97** 235416
[19] Xu Y *et al* 2000 *Nat. Commun.* **11** 3985
[20] Kane C L and Mele E J 2005 *Phys. Rev. Lett.* **95** 226801
[21] Furukawa N 1994 *J. Phys. Soc. Jpn.* **63** 3214
[22] Furukawa N 1994 *J. Phys. Soc. Jpn.* **64** 2754
[23] Furukawa N 1996 *J. Phys. Soc. Jpn.* **65** 1174
[24] Yunoki S, Hu J, Malvezzi A L, Moreo A, Furukawa N and Dagotto E 1998 *Phys. Rev. Lett.* **80** 845
[25] Kogan E and Auslender M 2003 *Phys. Rev.* B **67** 132410
[26] Phan V N and Tran M T 2003 *Mod. Phys. Lett.* B **17** 39
[27] Minh-Tien T 2003 *Phys. Rev.* B **67** 144404
[28] Phan V N and Tran M T 2005 *Phys. Rev.* B **72** 214418
[29] Phan V-N and Tran M-T 2015 *Phys. Rev.* B **92** 155201
[30] Phan V N, Ninh Q H and Tran M T 2016 *Phys. Rev.* B **93** 165115
[31] Tran M T, Nguyen H S and Le D A 2016 *Phys. Rev.* B **93** 155160
[32] Tran T T M, Le D A, Pham T M, Nguyen T K T and Tran M T 2020 *Phys. Rev.* B **102** 205124
[33] Wu F Y 1982 *Rev. Mod. Phys.* **54** 235
[34] Kohmoto M 1985 *Ann. Phys. (N.Y.)* **160** 355
[35] Thouless D J, Kohmoto M, Nightingale M P and den Nijs M 1982 *Phys. Rev. Lett.* **49** 405
[36] Seki K and Yunoki S 2016 *Phys. Rev.* B **93** 245115
[37] Metzner W and Vollhardt D 1989 *Phys. Rev. Lett.* **62** 324
[38] Ruderman M A and Kittel C 1954 *Phys. Rev.* **96** 99
[39] Kasuya T 1956 *Theor. Phys.* **16** 45
[40] Yosida K 1957 *Phys. Rev.* **106** 893
[41] Kassem M A, Tabata Y, Waki T and Nakamura H 2020 *J. Phys.: Condens. Matter* **33** 015801
[42] Kassem M A, Tabata Y, Waki T and Nakamura H 2017 *Phys. Rev.* B **96** 014429
[43] Moritomo Y, Akimoto T, Nakamura A, Ohoyama K and Ohashi M 1998 *Phys. Rev.* B **58** 5544